Sci

Article

Synthesis, Structural Characterization, and Biological Activities of Organically Templated Cobalt Phosphite $(C_4N_2H_{14})Co(H_2PO_3)_4{\cdot}2H_2O$

Najlaa Hamdi [1], Souad Chaouch [1], Ivan da Silva [2], Mohamed Ezahri [3], Mohammed Lachkar [1], Rama Alhasan [4], Ahmad Yaman Abdin [4], Claus Jacob [4] and Brahim El Bali [1]

[1] Engineering Laboratory of Organometallic and Molecular Materials, Faculty of Sciences, University Sidi Mohamed Ben Abdellah, Po. Box 1796 (Atlas), 30000 Fez, Morocco; hamdi.najlae@gmail.com (N.H.); chaouch2005@yahoo.fr (S.C.); lachkar.mohammed@gmail.com (M.L.); b_elbali@yahoo.com (B.E.B.)

[2] ISIS Facility, STFC Rutherford Appleton Laboratory, Chilton, Oxfordshire OX11 0QX, UK; ivan.da-silva@stfc.ac.uk

[3] Laboratoire Matériaux et Environnement, Faculté des Sciences, Université Ibn Zohr, B.P. 8106, Cité Dakhla, 80000 Agadir, Maroc; m.ezahri@uiz.ac.ma

[4] Department of Pharmacy, Building B 2.1, Room 1.13, Saarland State University, Saarbruecken, Germany; s8rralh@stud.uni-saarland.de (R.A.); yaman.ab@hotmail.com (A.Y.A.); c.jacob@mx.uni-saarland.de (C.J.)

* Correspondence: b_elbali@yahoo.com

Received: 17 January 2019; Accepted: 5 March 2019; Published: 12 March 2019 (Version 1, doi: 10.3390/sci1010013.v1)

Abstract: A novel hybrid phosphite $[(C_4N_2H_{14})Co(H_2PO_3)_4{\cdot}2H_2O]$ was synthesized with 1,4-diaminobutane (dabn) as a structure-directing agent using slow evaporation method. Single crystal X-ray diffraction analysis showed that it crystallizes in the triclinic system (S.G: P-1, #2) with the following unit cell parameters (Å, °) a = 5.4814 (3), b = 7.5515 (4), c = 10.8548 (6), α = 88.001 (4), β = 88.707 (5), γ = 85.126 (5). The crystal structure was built up from corner-sharing $[CoO_6]$-octahedrons, forming chains parallel to [001], which are interconnected by H_2PO_3 pseudo-pyramid units. The diprotonated 1,4-diaminobutane molecules, residing between the parallel chains, interacted with the inorganic moiety via hydrogen bonds leading thus to the formation of the 3D crystal structure. The Fourier transform infrared result exhibited characteristic bands corresponding to the phosphite group and the organic molecule. The thermal decomposition of the compound consists mainly of the loss of the organic moiety and the water molecules. The biological tests exhibited significant activity against *Candida albicans* and *Escherichia coli* strains in all used concentrations, while less activity was pronounced when tested against *Staphylococcus epidermidis* and *Saccharomyces cerevisiae*, while there was no activity against the nematode model *Steinernema feltiae.*

Keywords: hybrid phosphite; crystal structure; thermal behavior; biological activities; antimicrobial; micro-organisms

1. Introduction

Hybrid organic-inorganic materials have attracted a great deal of attention in different fields because of their rich structural chemistry and wide potential applications in ion-exchange, adsorption, separation, and catalysis [1–7]. Within this class of structures, hybrid phosphite continues to attract intense research attention from all facets of material scientists since it promoted the formation of a new range of structures with various architectures and dimensionality [8]. These materials might exhibit different types: simple (single metal) [9–12], mixed-metal [13–20] or hybrid (organic-inorganic)

[21,22]. In this context, we have described in the present paper the synthesis, crystal structure, spectroscopic characterization, and thermal behavior of the new hybrid phosphite $[(C_4N_2H_{14})Co(H_2PO_3)_4{\cdot}2H_2O]$. Moreover, we have reported on the biological activities, that is, its activity against *C. albicans*, *E. coli* strains, *S. epidermidis*, and *S. cerevisiae* as a first contribution in the investigations conducted by our research group on such research in the field of phosphite-phosphate materials.

2. Experimental

2.1. Synthesis

Single crystals of $[(C_4N_2H_{14})Co(H_2PO_3)_4{\cdot}2H_2O]$ were synthesized under ambient conditions. The reaction mixture of $Co(NO_3)_2{\cdot}6H_2O$ (1 mmol, 300 mg), 1,4-diaminobutane (dabn) (2 mmol, 170 mg), and H_3PO_3 (4 mmol, 300 mg) was shaken in distilled water for 6 h and then left at room temperature. After two weeks, the pink solution had concentrated and hexagonal purple crystals, which were harvested washed with the water-ethanol mixture (80:20) and dried in air.

2.2. Materials and Instrumentation

All reagents were acquired from commercial sources and used without further purification. The infrared spectrum of the compound was recorded on a VERTEX 70 FTIR Spectrometer in the range 4000–400 cm^{-1} using the ATR technique at 4 cm^{-1} resolution. Thermogravimetric analysis (TGA) data were recorded on an SDT-Q600 analyzer from TA Instruments (Eschborn, Germany). The temperature varied from RT to 1173 K at a heating rate of $10°/min^{-1}$. Measurements were carried out on samples in open platinum crucibles under air flow.

2.3. Crystal Structure Determination

Crystal Structure Determination

Single-crystal X-ray diffraction measurement was carried out at room temperature using an Agilent Gemini S diffractometer equipped with a CCD detector and molybdenum (Mo) radiation source. Acquired data were processed with the CrysAlisPro software [23]. Using Olex2 [24], the structure was solved with the olex2.solve [25] structure solution program using Charge Flipping and refined with the olex2.refine [25] refinement package using Gauss-Newton minimization. All non-hydrogen atoms were refined anisotropically, and hydrogen atoms were included in the model at calculated positions, refined with a rigid model with their Uiso value to 1.2Ueq of their parent atoms.

Table 1 reports the crystallographic data and experimental details of data collection and structure refinements. Atomic coordinates and equivalent thermal parameters are reported in Table 2, selected bond distances in Table 3. The structural graphics were created using both DIAMOND program [26] and Mercury [27].

Table 1. Experimental data collection details from $[(C_4N_2H_{14})Co(H_2PO_3)_4\cdot 2H_2O]$.

Chemical Formula/Mr (g/mol)	$[(C_4N_2H_{14})Co(H_2PO_3)_4\cdot 2H_2O]$/*509.08*
F(000)	263.9
Symmetry, S.G.	Triclinic (P-1, #2)
Cell parameters (Å, °)/V (Å^3)/Z	a = 5.4814 (3), b = 7.5515 (4), c = 10.8548 (6), α = 88.001 (4), β = 88.707 (5)°, γ = 85.126 (5)°/447.33 (4)/1
λ (Mo Kα radiation) (Å)	0.71073
T(K)/μ(mm^{-1})	298/1.39
Crystal sizes (mm)	0.25 × 0.25 × 0.3
Measured reflections/independent reflections (reflections with I ≥ 2u(I))/parameters	9480/2005 (1878)/137
θmin − θmax (°)/Rint	1.9–27.8/0.024
Reciprocal space	h: −6–7, k: −9–9, l: −13–14
R[F2 > 2σ(F2)]/wR(F2)/S	0.026/0.072/1.03

Table 2. Fractional atomic coordinates and displacement parameters (Å2) for the atoms in $[(C_4N_2H_{14})Co(H_2PO_3)_4\cdot 2H_2O]$ ("*" isotropic parameters for H atoms).

	x	**y**	**z**	**Uiso*/Ueq**
Co1	0.5	0	0.5	0.01218 (11)
P5	−0.02030 (8)	0.22049 (6)	0.42698 (4)	0.01422 (12)
H5	−0.007 (4)	0.111 (3)	0.344 (2)	0.021 (5) *
P7	0.52560 (9)	−0.06370 (6)	0.80899 (4)	0.01853 (13)
H7	0.634 (5)	−0.223 (3)	0.790 (2)	0.033 (6) *
O2	0.2188 (2)	−0.17568 (17)	0.48203 (12)	0.0186 (3)
O3	0.4308 (2)	0.01773 (18)	0.68967 (11)	0.0221 (3)
O4	0.2349 (2)	0.22465 (16)	0.47498 (12)	0.0183 (3)
O6	−0.0899 (3)	0.4083 (2)	0.36416 (14)	0.0276 (3)
H6	−0.234 (6)	0.439 (4)	0.365 (3)	0.051 (9) *
O8	0.6876 (3)	0.0461 (2)	0.87800 (13)	0.0335 (4)
O9	0.3019 (3)	−0.1124 (2)	0.89129 (13)	0.0346 (4)
H9	0.324 (2)	−0.087 (4)	0.9627 (5)	0.0519 (6) *
O13	−0.5521 (3)	0.5209 (2)	0.35642 (15)	0.0261 (3)
H13a	−0.574 (6)	0.602 (4)	0.387 (3)	0.044 (9) *
H13b	−0.607 (5)	0.442 (4)	0.388 (2)	0.030 (7) *
N12	0.0271 (3)	0.2595 (2)	0.77025 (14)	0.0220 (3)
H12a	−0.027 (2)	0.3488 (2)	0.7196 (6)	0.0264 (4) *
H12b	0.1433 (7)	0.1909 (15)	0.7321 (7)	0.0264 (4) *
H12c	−0.0966 (17)	0.1953 (15)	0.79227 (19)	0.0264 (4) *
C10	−0.0486 (4)	0.4687 (3)	0.94033 (18)	0.0263 (4)
H10a	−0.2031 (4)	0.4179 (3)	0.95693 (18)	0.0316 (5) *
H10b	−0.0785 (4)	0.5696 (3)	0.88336 (18)	0.0316 (5) *
C11	0.1294 (4)	0.3320 (3)	0.88205 (18)	0.0264 (4)
H11a	0.1693 (4)	0.2355 (3)	0.94144 (18)	0.0316 (5) *
H11b	0.2794 (4)	0.3857 (3)	0.85960 (18)	0.0316 (5) *

Table 3. Basic geometrical data from [$(C_4N_2H_{14})Co(H_2PO_3)_4{\cdot}2H_2O$].

Co1—O2	2.1336 (12)	P5—O6	1.5732 (14)
Co1—O2i	2.1336 (12)	P7—O3	1.4987 (13)
Co1—O3	2.0919 (12)	P7—O8	1.4955 (15)
Co1—O3i	2.0919 (12)	P7—O9	1.5625 (15)
Co1—O4i	2.1519 (12)	N12—C11	1.489 (2)
Co1—O4	2.1519 (12)	C10—C10iii	1.517 (4)
P5—O2ii	1.5050 (13)	C10—C11	1.505 (3)
P5—O4	1.5067 (13)		
O2i—Co1—O2	180	O4—Co1—O3	87.41 (5)
O3i—Co1—O2	88.26 (5)	O4i—Co1—O4	180
O3—Co1—O2	91.74 (5)	O4—P5—O2ii	117.53 (7)
O3—Co1—O2i	88.26 (5)	O6—P5—O2ii	109.58 (8)
O3i—Co1—O2i	91.74 (5)	O6—P5—O4	106.61 (8)
O3i—Co1—O3	180	O8—P7—O3	115.59 (9)
O4—Co1—O2i	90.01 (5)	O9—P7—O3	108.23 (8)
O4—Co1—O2	89.99 (5)	O9—P7—O8	110.69 (8)
O4i—Co1—O2i	89.99 (5)	P5ii—O2—Co1	129.16 (7)
O4i—Co1—O2	90.01 (5)	P7—O3—Co1	139.61 (8)
O4i—Co1—O3i	87.41 (5)	P5—O4—Co1	126.28 (7)
O4i—Co1—O3	92.59 (5)	C10—C11—N12	111.66 (16)
O4—Co1—O3i	92.59 (5)		

Symmetry codes: (i) $-x + 1, -y, -z + 1$; (ii) $-x, -y, -z + 1$; (iii) $-x, -y + 1, -z + 2$.

Supplementary tables of crystal structures and refinements, notably the full list of bond lengths and angles, and anisotropic thermal parameters were deposited with the Inorganic Crystal Structure Database, FIZ, Hermann von Helmholtz Platz 1, 76344 EggensteinLeopoldshafen, Germany; fax: (+49) 7247 808 132; Email: crysdata@fiz-karlsruhe.de. Deposition number is CCDC 1882579.

2.4. Biological Activities

2.4.1. Nematicidal Activity

The model nematode *Steinernema feltiae* was purchased from Sautter und Stepper GmbH (Ammerbuch, Germany) in the form of powder and stored at 4 °C in the dark. Fresh samples were utilized prior to each experiment. A homogeneous mixture was prepared by dissolving 200 mg of nematode powder in 50 mL distilled water. Later on, the nematode suspension was placed for 15 min at room temperature with shaking and in moderate light. Viability was examined under a light microscope at four-fold magnification (TR 200, VWR International, Leuven, Belgium). The viability of nematodes above 80% in each sample was considered a prerequisite for each experiment. Ten microliters of nematode suspension were added to each well of a 96-well plate. The hybrid cobalt phosphite [$(C_4N_2H_{14})Co(H_2PO_3)_4{\cdot}2H_2O$] was then added into the wells to achieve final concentrations of 250, 500, and 1000 μM. Afterward, the final volume in each well was adjusted to 100 μL by adding Phosphate Buffered Saline (PBS pH = 7.4). PBS and ethanol (10 μL per well) were employed as negative and positive controls, respectively, and sterile distilled water was the solvent control. Each experiment was performed independently on three different occasions and in triplicate ($n = 9$). Living and dead nematodes were counted under the microscope prior to treatment, and the viability fraction (V0) was calculated (usually >0.9). Then, 50 μL of lukewarm water (40 °C) was added to each well to stimulate the nematodes prior to counting. After 24 h, the V24 fraction was calculated, by once more counting the living and dead nematodes, and expressed as a percentage of initial viability V0 according to the equation:

$$\text{Viability (\%)} = [V_{24}/V_0] \times 100$$

Results are represented as mean ± SD, and GraphPad Prism (Version 5.03, GraphPad Software, La Jolla, CA, USA) was used to calculate the statistical significances by one-way ANOVA. $p < 0.05$ was considered to be statistically significant.

2.4.2. The Antimicrobial Activity

This section may be divided by subheadings. It should provide a concise and precise description of the experimental results, their interpretation, as well as the experimental conclusions, that can be drawn. The activity of $[(C_4N_2H_{14})Co(H_2PO_3)_4{\cdot}2H_2O]$ compound against *Escherichia coli*, *Staphylococcus epidermidis*, *Candida albicans*, and *Saccharomyces cerevisiae* was investigated in routine microbial growth assays based on optical density and recorded in the form of growth curves. Fresh cultures of *S. epidermidis*, *E. coli*, *C. albicans*, and *S. cerevisiae* were prepared on bacterial tryptic soy broth, Luria-Bertani broth (LB), Sabouraud Dextrose Agar (SDA), and Yeast Peptone Dextrose (YPD) agar media, respectively. After 18–24 h of incubation, the microbial colonies from these Agar plates were then transferred into 10 mL solution of 0.9% *w*/*v* NaCl (saline), and the turbidity of the suspension was adjusted to 0.5 of McFarland standard. These microbial suspensions were then exposed to the samples as described below. Bacterial and yeast culture with growth medium were employed as negative control, sterile distilled water was utilized as solvent control, while the positive control consisted of a mixture of 10,000 units/mL of penicillin, 10,000 µg/mL of streptomycin, and 25 µg/mL of amphotericin B. The sample was evaluated at various dilutions (of 250, 500, and 1000 µM), and the plates were incubated at 37 °C for 24 h. Microbial growth was monitored by recording the optical density of the samples at 0 h and 24 h, using a Micro Plate Reader E800 at 593 nm. These absorbance values were converted into percentages and compared to the negative control whose absorbance values were normalized to 100% and served as references at each time interval. All experiments were carried out in triplicate at three different occasions ($n = 9$). Results are represented as mean ± SD, and statistical significances were calculated by one-way ANOVA using GraphPad Prism (Version 5.03, GraphPad Software, La Jolla, CA, USA) with $p < 0.05$ considered to be of statistical significance.

3. Results and Discussion

3.1. Structural Description

As shown in Figure 1, there is one crystallographically distinct site for Co atom in the asymmetric unit of $[(C_4N_2H_{14})Co(H_2PO_3)_4{\cdot}2H_2O]$ which contains 13 non-hydrogen atoms. The six coordinated cobalt exhibits octahedral geometry by oxygen donors from the adjacent phosphite groups. The Co–O bond lengths range from 2.0920 (1) Å to 2.1336 (1) Å with an average Co–O distance of 2.1258 Å, a comparable value to that of 2.113 Å reported in $[(C_4N_8H_{12})Co(HPO_3)_2(C_2O_4)_3]$ [28] and to that of 2.101 Å for $NaCo(H_2PO_3)_3{\cdot}H_2O$ [29]. All H_2PO_3 units adopt pseudo pyramidal coordination geometry. P(5) shares two oxygen with adjacent Co atoms, while P(7) is connected by one P–O–Co bond and possesses a short terminal P–O bond (1.4945 (1) Å). The P–O bond distances are in the range 1.5049(1)–1.5372 (1) Å for P(5) atom [Av. 1.5282 Å] and 1.495 (1)–1.506 (1) Å for P(7) [Av. 1.499 Å]. P(5) and P(7) atoms have a terminal phosphite P–H bond 1.241 (1) and 1.3127 (1) Å, respectively. These values are of the usual magnitude as the ones reported in $(C_2NH_8)_2[Co_3(HPO_3)_4]$, $(C_4N_2H_{12}[Co(HPO_3)_2]$ [30], and $(C_6H_{16}N_2)[Co(HPO_3)F]$ [31]. The strict alternation of CoO_6 octahedra and H_2PO_3 pseudo pyramids via oxygen vertices results in an anionic network with a Co/P ratio of 1/2. The polyhedral units are joined through corners sharing four-membered rings, which are thereby connected through their edges forming an infinite one-dimensional chain rising along [100] (Figure 2). The individual chain units are further linked together through hydrogen bond interactions (Figure 3, Table 4). The 1,4-diaminobutane templates, which reside between the parallel chains, are diprotonated. They are further ensuring, together with the free water molecules, the stability of the three-dimensional network.

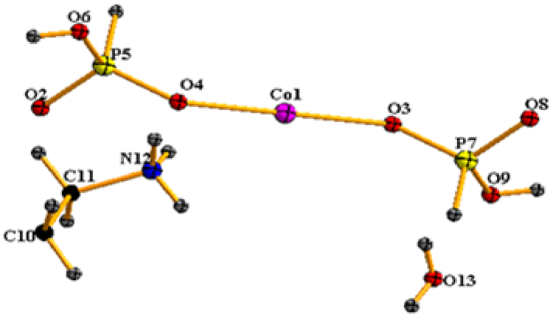

Figure 1. The asymmetric unit of [($C_4N_2H_{14}$)Co(H_2PO_3)$_4$·2H_2O]. Thermal ellipsoids are shown at 50% probability.

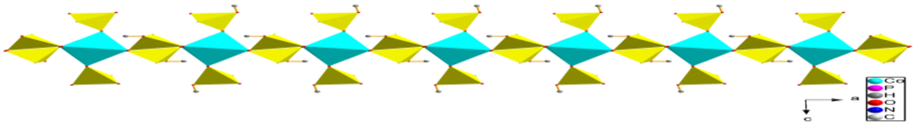

Figure 2. A fragment of the structure of [($C_4N_2H_{14}$)Co(H_2PO_3)$_4$·2H_2O] along [010], showing the infinite four-membered ring chain propagating along [100].

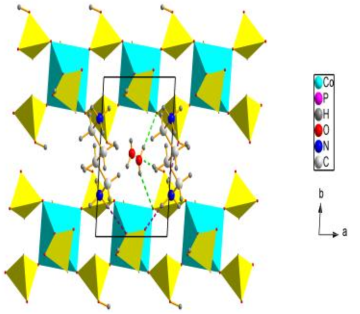

Figure 3. The crystal structure of [($C_4N_2H_{14}$)Co(H_2PO_3)$_4$·2H_2O] in a projection along c-axis emphasizing the hydrogen bonds (dashed lines).

Table 4. H-bonds distances in the framework of [($C_4N_2H_{14}$)Co(H_2PO_3)$_4$·2H_2O].

D-H···A	D-H/Å	H···A/Å	D···A/Å	Angle DHA/°
O6-H6···O13	0.80 (3)	1.80 (3)	2.605 (2)	175 (3)
O9-H9···O8	0.819 (10)	1.766 (8)	2.574 (2)	168.5 (16)
N12-H12A···O6	0.890 (5)	2.158 (5)	2.900 (2)	140.3 (9)
N12-H12B···O3	0.890 (8)	2.016 (8)	2.887 (2)	165.5 (7)
N12-H12C···O8	0.890 (10)	1.907 (9)	2.776 (2)	164.8 (5)
O13-H13A···O2	0.71 (3)	2.22 (3)	2.888 (2)	159 (3)
O13-H13B···O4	0.76 (3)	2.11 (3)	2.863 (2)	179 (4)

3.2. Infrared Spectroscopy

The infrared spectrum of [($C_4N_2H_{14}$)Co(H_2PO_3)$_4$·2H_2O] (Figure 4) exhibits bands corresponding to the vibration modes of the organic template and phosphite groups. The stretching vibration of NH_2 in dabn cation is observed in the high frequencies 3090–3200 cm^{-1}, while its bending appears at 1600 cm^{-1} [32]. The values at around 2850 and 1300 cm^{-1} are boil down to the stretching vibration of CH2 and C–N, respectively. The band appearing at 2450 cm^{-1} corresponds to the stretching vibration of P–H bond which is the characteristic bond of phosphite groups, whereas the bands from 990 to 1030 cm^{-1} are assigned to the bending mode of P–H. The vibration modes centered at 570, 1050, and 1160 cm^{-1} are ascribed to the stretching vibration of PO_3 group, while the one located at 910 cm^{-1} presents the stretching vibration of P–OH [20]. The set of bands related to the stretching vibration and deformation of the OH group belonging to water molecules is observed at around 3000 and 1640 cm^{-1} [33,34].

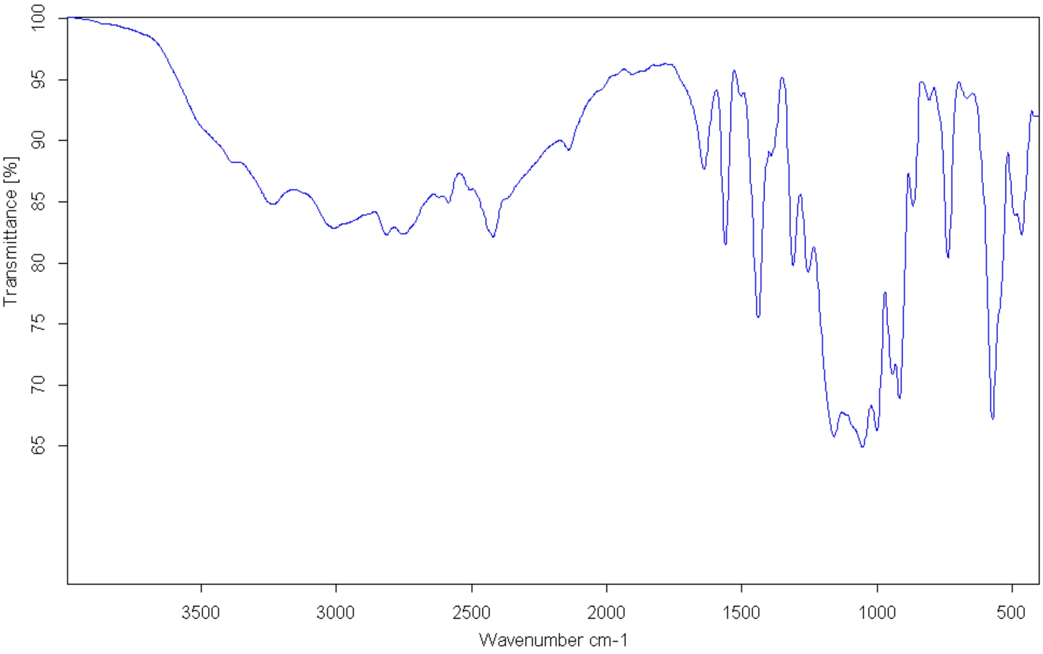

Figure 4. The infrared spectrum of [($C_4N_2H_{14}$)Co(H_2PO_3)$_4$·2H_2O].

3.3. Thermal Behavior

TGA experiment was performed under an air atmosphere. The experimental data, given from TG analysis (Figure 5), show three separated steps of weight loss in a total of 45% for [($C_4N_2H_{14}$)Co(H_2PO_3)$_4$·2H_2O]. The first mass loss of 10% in the range of 180–220 °C is accompanied by an endothermic signal in the differential thermal analysis (DTA) trace at 180 °C. The peak coincidences with the departure of 1.5 water molecules (calculated mass 9.8%). The second stage with a theoretical weight loss of 8% starting at about 320 °C and ending at 420 °C can be related to the decomposition of 1,4-diaminobutane (calculated weight loss 8%). This phenomenon is coupled with an exothermic heat flow noticed at 340 °C. The total decomposition of the organic moiety and the remaining water molecules is shown between 540–660 °C (observed weight loss 27%), with a small exothermic curve at 640 °C (calculated weight loss 27.8%).

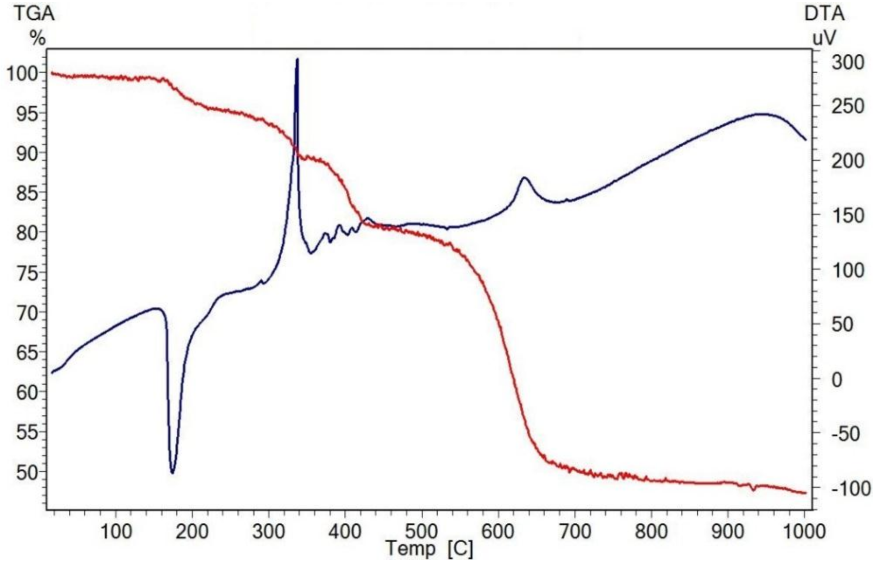

Figure 5. Thermogravimetric (TG) and differential thermal analysis (TDA) curves of $[(C_4N_2H_{14})Co(H_2PO_3)_4{\cdot}2H_2O]$.

3.4. Biological Activities

The hybrid cobalt phosphite compound was tested for their antimicrobial activity against two bacterial (*Escherichia coli* and *Staphylococcus epidermidis*) and two fungal (*Saccharomyces cerevisiae* and *Candida albicans*) strains. The mixture of 10,000 units/mL of penicillin, 10,000 µg/mL of streptomycin, and 25 µg/mL of Amphotericin B was used as control drugs. The percentage inhibition and minimum inhibitory concentration (MIC) values of the compound based on the growth of microorganisms are shown in Figure 6a. The highest inhibition activity of the compound was observed against *C. albicans* fungi with a MIC value of 500 $\mu g{\cdot}mL^{-1}$. The compound showed a lower activity against *E. coli* (1000 $\mu g{\cdot}mL^{-1}$) than positive control, while no significant activity was observed against *S. cerevisiae* and *S. epidermidis* strains.

The nematicidal activity of $(C_4N_2H_{14})Co(H_2PO_3)_4$ was investigated against *S. feltiae* nematode. Ethanol was used as a positive control. No mortality of nematodes was observed; such a result indicates that the hybrid compound was inactive against *S. feltiae* (Figure 6b).

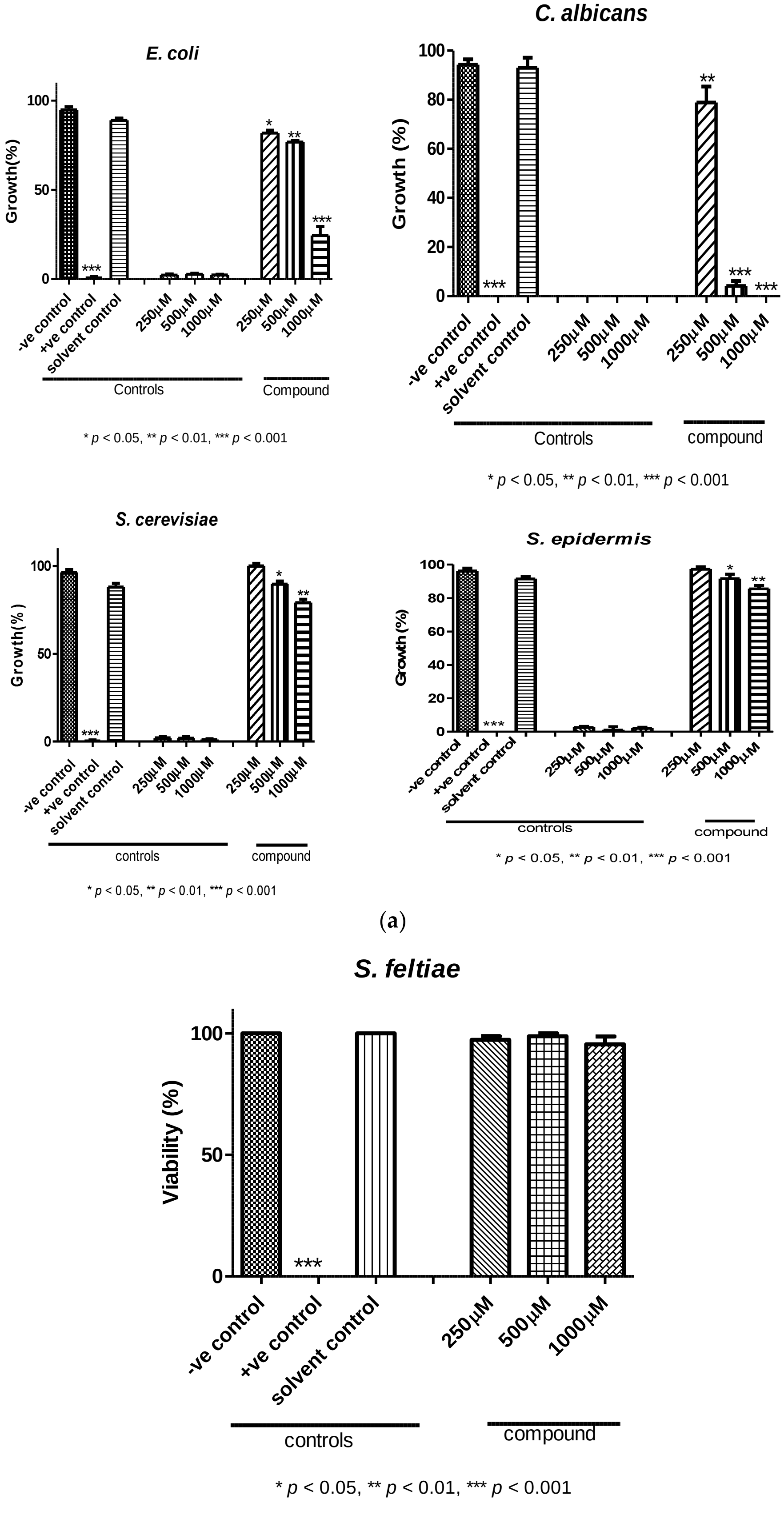

(a)

(b)

Figure 6. Antibacterial activity of $[(C_4N_2H_{14})Co(H_2PO_3)_4$ against bacterial and fungal strains (**a**) and *S. feltiae* nematode (**b**).

4. Conclusions

New organically templated cobalt phosphite [($C_4N_2H_{14}$)Co(H_2PO_3)$_4$·2H_2O] has been synthesized using wet chemistry. Single crystal structure analysis revealed that the framework displays a one dimensional (1D) chain-like structure, containing vertex sharing four-membered rings formed by the connectivity between CoO_6 octahedrons and H_2PO_3 pseudo pyramid units bound through their edges. The diprotonated 1,4-diaminobutane acts as a stabilizer of the inorganic network through hydrogen bonds. The thermogravimetric analysis showed that the dehydration of the hybrid phosphite takes place in three steps, resulting mainly from the loss of the organic moiety and water molecules. The antimicrobial investigation showed significant activity against some microorganisms, that is, *C. albicans* and almost no activity against *S. feltiae*, suggesting that the activity of the compound is related to the type of the studied microorganisms.

Author Contributions: Najlaa Hamdi performed the experiments and started writing the manuscript as part of her thesis report, Souad Chaouch supported her under the supervision of Mohammed Lachkar. Ivan da Silva solved the crystal structure. Mohamed Ezahri measured the thermal features of the material, Rama Alhasan, Ahmad Yaman Abdin and Claus Jacob achieved the biological tests and wrote the corresponding part of the manuscript. Brahim El Bali planned the research, rewrote the crystal structure part and finalized writing the manuscript.

Funding: This research had no external funding!

Acknowledgments: The authors would like to acknowledge the support and technical assistance of Interface Regional University Center (Sidi Mohammed Ben Abdellah University, Fez) and National Center for Scientific and Technical Research (CNRST-Rabat). Mrs. Alhasan would like to acknowledge Dahye Kim and Hyemin Oh from Ewha Womans University (South Korea) for their participation in the biological activities tests.

Conflicts of Interest: The authors declare no conflict of interest.

References

1. Garcia-Fernandez, A.; Bermudez-Garcia, J.M.; Castro-Garcia, S.; Artiaga, R.; Lopez-Beceiro, J.; Senaris-Rodriguez, M.A.; Sanchez-Andujar, M. Dielectric properties induced by the framework in the hybrid organic-inorganic compounds M(dca)2pyz M= Fe, Co and Zn. *Polyhedron* **2016**, *114*, 249–255.
2. Xiong, D.B.; Li, M.R.; Liu, W.; Chen, H.H.; Yang, X.X.; Zhao, J.T. Synthesis, structure and luminescence property of two lanthanum phosphite hydrates: La-2(H_2O)(x)(HPO_3)(3) (x=1,2). *J. Solid State Chem.* **2006**, *179*, 2571–2577.
3. Wang, L.; Song, T.; Fan, Y.; Tian, Z.; Wang, Y.; Shi, S.; Xu, J. Synthesis and characterization of a new open-framework fluorinated gallium phosphite with three-dimensional intersecting channels. *J. Solid State Chem.* **2006**, *179*, 3400–3405.
4. Chung, U.C.; Mesa, J.L.; Pizarro, J.L.; Jubera, V.; Lezama, L.; Arriortua, M.I.; Rojo, T. Mn(HPO_3): A new manganese (II) phosphite with a condensed structure. *J. Solid State Chem.* **2005**, *178*, 2913–2921.
5. Shi, S.H.; Qian, W.; Li, G.H.; Wang, L.; Yuan, H.M.; Xu, J.N.; Zhu, G.S.; Song, T.Y.; Qiu, S.L. Building three-dimensional metal phosphites from the corner-shared four-membered rings chain. *J. Solid State Chem.* **2004**, *177*, 3038–3044.
6. Lin, Z.E.; Fan, W.; Gao, F.; Chino, N.; Yokoi, T.; Okubo, T. A novel layered bimetallic phosphite intercalating with organic amines: Synthesis and characterization of Co(H_2O)$_4$Zn$_4$(HPO_3)$_6$.$C_2N_2H_{10}$. *J. Solid State Chem.* **2006**, *179*, 723–728.
7. Zhong, Y.J.; Chen, Y.M.; Sun, Y.Q.; Yang, G.Y. Syntheses and characterization of two new zinc phosphites with 1D chains decorated by Zn-centered complexes. *J. Solid State Chem.* **2005**, *178*, 2613–2619.

8. Agarwal, R.A.; Mukherjee, S. One dimensional coordination polymers of Cd(II) and Zn(II): Synthesis, structure, polar packing through strong inter-chain hydrogen bonding and gas adsorption studies. *Polyhedron* **2016**, *106*, 163–170.
9. Ouarsal, R.; Tahiri, A.A.; El Bali, B.; Lachkar, M.; Bolte, M. Strontium dihydrogenphosphite. *Acta Crystallogr.* **2002**, *E58*, i19–i20.
10. Ouarsal, R.; Tahiri, A.A.; Lachkar, M.; Slimani, Z.; El Bali, B.; Bolte, M. Barium dihydrogen phosphate hemihydrates. *Acta Crystallogr.* **2002**, *E58*, i72–i73.
11. Chaouche, S.; Ouarsal, R.; El Bali, B.; Lachkar, M.; Bolte, M.; Dusek, M. Li_2HPO_3 H_2O: Crystal Structure and IR Spectrum. *J. Chem Crystallogr.* **2010**, *40*, 526–530.
12. El Bali, B.; Massa, W. Redetermination of copper(II) hydrogenphosphite dehydrate. *Acta Crystallogr.* **2002**, *E58*, i29–i31.
13. Chaouch, S.; Ouarsal, R.; Akouibaa, M.; Rakib, S.; Lachkar, M.; El Bali, B.; Dusek, M. $Cs_2[M(H_2O)_6]_3(HPO_3)_4$, M= Co, Ni: Crystal structures, IR and thermal studies. *J. Phys. Conf. Ser.* **2018**, *984*, 12–15.
14. Ouarsal, R.; Tahiri, A.A.; El Bali, B.; Lachkar, M.; Harrison, W.T.A. Sodium zinc tris(dihydrogenphosphite) hydrate $NaZn(H_2PO_3)_3.H_2O$. *Acta Crystallogr.* **2002**, *E58*, i23–i25.
15. Ouarsal, R.; Tahiri, A.A.; Lachkar, M.; Dusek, M.; Fejfarová, K.; El Bali, B. Sodium magnesium tris(dihydrogenphosphite)monohydratehydrate, $NaMg(H_2PO_3)_3$ H_2O. *Acta Crystallogr.* **2003**, *E59*, i33–i35.
16. Ouarsal, R.; Essehli, R.; Lachkar, M.; Zenkouar, M.; Dusek, M.; Fejfarová, K.; El Bali, B. Dipotassium cobalt(II) bis(hydrogenphosphite) dihydrate, $K_2Co(HPO_3)_2,2H_2O$. *Acta Crystallogr.* **2004**, *E60*, i66–i68.
17. Messouri, I.; El Bali, B.; Capitelli, F.; Piniella, J.F.; Lachkar, M.; Slimani, Z. Diammoniumtris[hexaaquamagnesium(II)]tetrakis[hydrogenphosphate(III)], $(NH_4)_2[Mg(H_2O)_6]_3(HPO_3)_4$. *Acta Crystallogr.* **2005**, *E61*, i129–i131.
18. Ouarsal, R.; El Bali, B.; Lachkar, M.; Dusek, M.; Fejfarová, K. Diammoniumtris[hexaaquanickel(II)]tetrakis[hydrogenphosphate(III)], $(NH_4)_2[Ni(H_2O)_6]_3(HPO_3)_4$. *Acta Crystallogr.* **2005**, *E61*, i171–i173.
19. Ouarsal, R.; El Bali, B.; Lachkar, M.; Dusek, M.; Fejfarová, K. Diammonium tris[hexaaquacobalt(II)] tetrakis[hydrogenphosphate(III)], $(NH_4)_2[Co(H_2O)_6]_3(HPO_3)_4$. *Acta Crystallogr.* **2005**, *E61*, i168–i170.
20. Ouarsal, R.; Lachkar, M.; Dusek, M.; Albert, E.B.; Castelló, J.B.C.; El Bali, B. Crystal structure of $NaCd(H_2PO_3)_3$ H_2O and spectroscopic study of $NaM(H_2PO_3)_3$ H_2O, M = Mn, Co, Ni, Zn, Mg and Cd. *Polyhedron*. **2016**, *106*, 132–137.
21. Chaouche, S.; Ouarsal, R.; Lachkar, M.; Capitelli, F.; El Bali, B. Crystal Structure and IR Study of $(C_6H_5NH_3)[ZnCl(HPO_3)]$. *J. Chem Crystallog.* **2010**, *40*, 486–490.
22. Suhua, S.; Wei, Q.; Guanghua, L.; Li, W.; Hongming, Y.; Jianing, X.; Zhu, G.; Song, T.; Qiu, S.J. Building three-dimensional metal phosphites from the corner-shared four-membered rings chain. *Solid State Chem.* **2004**, *177*, 3038–3044.
23. *CrysAlisPro Software System*, version 1.171.38.41; Rigaku Corporation: Oxford, UK, 2015.
24. Dolomanov, O.V.; Bourhis, L.J.; Gildea, R.J.; Howard, J.A.K.; Puschmann, H. OLEX2: A complete structure solution, refinement and analysis program. *J. Appl. Cryst.* **2009**, *42*, 339–341.
25. Bourhis, L.J.; Dolomanov, O.V.; Gildea, R.J.; Howard, J.A.K.; Puschmann, H. The anatomy of a comprehensive constrained, restrained refinement program for the modern computing environment—*Olex2* dissected. *Acta Cryst. A* **2015**, *71*, 59–75.
26. Brandenburg, K.; Putz, H. *DIAMOND Version 3*; Crystal Impact GbR: Bonn, Germany, 2005.

27. Macrae, C.F.; Bruno, I.J.; Chisholm, J.A.; Edgington, P.R.; McCabe, P.; Pidcock, E.; Rodriguez-Monge, L.; Taylor, R.; Van de Streek, J.; Wood, P.A. Mercury CSD 2.0—New Features for the Visualization and Investigation of Crystal Structures. *J. Appl. Cryst.* **2008**, *41*, 466–470.
28. Mandal, S.; Natarajan, S. Inorganic–organic hybrid structure: Synthesis, structure and magnetic properties of a cobalt phosphite–oxalate, $[C_4N_2H_{12}][Co_4(HPO_3)_2(C_2O_4)_3]$. *J. Solid State Chem.* **2005**, *178*, 2376–2382.
29. Kratochvıl, B.; Podlahova, J.; Habibpur, S.; Petricek, V.; Maly, K. Cobalt(II) sodium dihydrogenphosphite monohydrate. *Acta Cryst.* **1982**, *B38*, 2436–2438.
30. Liu, X.; Xing, Y.; Liu, X. Solvothermal synthesis and magnetic properties of cobalt(II) phosphite structures of varying dimensionality. *Cryst. Eng. Commun*. **2010**, *12*, 383–386.
31. Fernández-Armas, S.; Mesa, J.L.; Pizarro, J.L.; Chung, U.C.; Arriortua, M.I.; Rojo, T. Two new two-dimensional organically templated phosphite compounds: $(C_6H_{16}N_2)_{0.5}[M(HPO_3)F]$, M=Fe(II) and Co(II): Solvothermal synthesis, crystal structures, thermal, spectroscopic, and magnetic properties. *J. Solid State Chem.* **2005**, *178*, 3554–3562.
32. Kantarcı, Z.; Sag lam, S.; Kasap, E. Vibrational spectroscopic studies on the 1,4-diaminobutane-T_d-type clathrates: $Cd(dabn)M(CN)_4 \cdot 1,5C_6H_6$ (M=Cd or Hg). *Spectrosc. Lett.* **2002**, *35*, 811–819.
33. Novak, A. Hydrogen bonding in solids correlation of spectroscopic and crystallographic data. In *Large Molecules. Structure and Bonding*; Springer: Berlin/Heidelberg, Germany, 1974; pp. 177–216.
34. Gilli, G.; Gilli, P. Towards a Unified Hydrogen-Bond Theory. *J. Mol. Struct.* **2000**, *552*, 1–15.